BBA - Biomembranes 1863 (2021) 183665

Contents lists available at ScienceDirect

BBA - Biomembranes

journal homepage: www.elsevier.com/locate/bbamem

New short cationic antibacterial peptides. Synthesis, biological activity and mechanism of action

Beatriz Lima [a], Maria Ricci [b], Adriana Garro [c], Tünde Juhász [b], Imola Csilla Szigyártó [b], Zita I. Papp [d], Gabriela Feresin [a], Jose Garcia de la Torre [e], Javier Lopez Cascales [f], Lívia Fülöp [d,1], Tamás Beke-Somfai [b,1], Ricardo D. Enriz [c,*,1]

[a] Instituto de Biotecnología, Universidad Nacional de San Juan, Av. Libertador General San Martín 1109 (O), CP 5400 San Juan, Argentina
[b] Research Centre for Natural Sciences, Institute of Materials and Environmental Chemistry, H-1117 Budapest, Hungary
[c] Facultad de Química, Bioquímica y Farmacia, Universidad Nacional de San Luis, Instituto Multidisciplinario de Investigaciones Biológicas (IMIBIO-SL), Chacabuco 915, 5700 San Luis, Argentina
[d] Department of Medical Chemistry, University of Szeged, H-6720 Szeged, Dóm tér 8, Hungary
[e] Facultad de Química, Departamento de Química Física, Universidad de Murcia, Campus de Espinardo, 30100 Espinardo, Murcia, Spain
[f] Grupo de Bioinformática y Macromoléculas (BioMac), Área de Química Física, Universidad Politécnica de Cartagena, Aulario II,· Campus de Alfonso XIII, 30203 Cartagena, Murcia, Spain

ARTICLE INFO

Keywords:
Antimicrobial peptides
Small-sized peptides
Mechanism of action
Peptide biophysical characterization

ABSTRACT

We report a theoretical and experimental study on a new series of small-sized antibacterial peptides. Synthesis and bioassays for these peptides are reported here. In addition, we evaluated different physicochemical parameters that modulate antimicrobial activity (charge, secondary structure, amphipathicity, hydrophobicity and polarity). We also performed molecular dynamic simulations to assess the interaction between these peptides and their molecular target (the membrane). Biophysical characterization of the peptides was carried out with different techniques, such as circular dichroism (CD), linear dichroism (LD), infrared spectroscopy (IR), dynamic light scattering (DLS), fluorescence spectroscopy and TEM studies using model systems (liposomes) for mammalian and bacterial membranes. The results of this study allow us to draw important conclusions on three different aspects. Theoretical and experimental results indicate that small-sized peptides have a particular mechanism of action that is different to that of large peptides. These results provide additional support for a previously proposed four-step mechanism of action. The possible pharmacophoric requirement for these small-sized peptides is discussed. Furthermore, our results indicate that a net +4 charge is the adequate for 9 amino acid long peptides to produce antibacterial activity. The information reported here is very important for designing new antibacterial peptides with these structural characteristics.

1. Introduction

The increasingly serious problem of resistance to many antibiotics of medicinal use has reduced the effectiveness of these essential therapeutic agents [1–4]. An example is the appearance of resistance to methicillin and vancomycin [5–8], an increasingly serious worldwide problem that requires an immediate solution. Many organisms, including humans, produce a number of broad-range antimicrobial peptides (AMPs). When these peptides are secreted on the surface of the epithelium they mount a powerful defense, providing a physical barrier separating the organism from the environment. They do not have a specific molecular target or process (as antibiotics), but act on cell membranes leading to cell lysis and death through rupture or alteration of the membrane topology. Thus, AMPs are highly effective ancient weapons used by different organisms to combat microbial infections [9,10]. There is a vast number of AMPs reported to date, with more than 5000 characterized sequences [11]. Having membranes as a molecular target has some advantages over standard antibiotics, but also entails some disadvantages. The main advantage is the great structural variety of these peptides that can produce antibacterial effects which

* Corresponding author.
E-mail addresses: fulop.livia@med.u-szeged.hu (L. Fülöp), beke-somfai.tamas@ttk.mta.hu (T. Beke-Somfai), denriz@unsl.edu.ar (R.D. Enriz).
[1] These authors share equal senior authorship.

https://doi.org/10.1016/j.bbamem.2021.183665
Received 3 February 2021; Received in revised form 7 May 2021; Accepted 1 June 2021

subsequently reduces the possibility of developing resistance [9,12]. Regarding the disadvantages, some AMPs suffer from a variety of pharmacokinetic shortcomings, including poor bioavailability, low metabolic stability and formulation difficulties due to their size. Additionally, in the case of long peptides, the process of synthesis is a significant problem when trying to convert them into commercial agents.

Due to the great structural variety of AMPs it is very difficult to make a single classification or categorization. However, there are common structural characteristics that deserve to be highlighted. In general, they have a net positive charge of at least +2 (and usually ranging between +3 to +5), amphipathic chains, residues with a length ranging between 10 and 40 [4] and many have secondary structures type α-helices or β-sheet, although extended and loop structures have also been determined in some cases. A wide spectrum of short cationic AMPs, defined as intrinsically disordered (ID), have no distinct secondary structure in aqueous solution due to electrostatic repulsion between charged residues [13–15]. However, when interacting with negatively charged natural or model membranes, they fold into β-sheets or amphiphilic helical structures and this conformational transition is often crucial for destabilizing the membrane and thus executing their biological activity [16,17]. Moreover, it has been suggested that membrane insertion of small-size peptides occurs above a critical concentration threshold and peptide self-assembly is an essential requisite for pore formation [18]. Structural diversity indicates that the mechanism of action of these peptides on the membrane is complex and goes beyond the mechanism of pore formation produced by helical structures or the so-called carpet mechanism [19,20].

On the other hand, from a practical point of view, one limitation for the therapeutic use of antibacterial peptides is the high costs associated with the synthesis of long-sized peptides. In addition, their well-known pharmacokinetic problems seriously reduce their potential therapeutic utility. An alternative is the development of peptides with 9–11 residues with antibacterial activity. Indeed, numerous studies have been carried out on the efficacy of short-sized peptides which have led to the discovery of several short active cationic antimicrobial peptides [21]. Our research group has reported a number of short-sized peptides with significant antimicrobial activities, both antibacterial [22,23] and antifungal [24–28].

Regarding the possible mechanisms of action, there are numerous studies and reviews on the mechanism of action of large AMPs such as defensin [29–31], melittin and other peptides of similar size [19,32]. There are also widespread mechanistic studies on peptides with an "intermediate" size such as protegrin-3 [33]. Penetratin is also included within this group of intermediate-sized peptides. Although penetratin is a well-known cell-penetrating agent, antifungal [34,35] as well as antibacterial activity have been also reported for this peptide [36,37]. In contrast, there are very few studies on the possible mechanism of action of peptides with less than 11 amino acids [38]. It is important to note, that the results of Liu et al. [38] suggest that these short peptides probably do not share the same mode of action as for large peptides. Our research group has previously reported a possible mechanism of action for these short-sized peptides based on molecular dynamics simulation (MDS) [39]. In the present paper, we report a theoretical-experimental study on a new series of small-sized AMPs (Table 1), focusing especially on their mechanism of action at the molecular level. Different physicochemical parameters modulating antimicrobial activity (charge, secondary structure, hydrophobicity, amphipathicity and polarity) were evaluated. The biophysical characterization of peptides was carried out using different techniques, such as circular dichroism (CD), linear dichroism (LD), infrared spectroscopy (IR), dynamic light scattering (DLS) and fluorescence spectroscopy, as well as model systems for mammalian and bacterial membranes.

2. Methods

2.1. Peptide synthesis

Synthesis of peptides 1 and 2 was already reported in our previous works, details about synthesis procedures can be obtained from references [24] and [26], respectively. Synthesis of peptides 3–9 was carried out as follows: solid phase synthesis of the peptides was carried out manually using an Fmoc Rink Amide AM resin (100–200 mesh, 0.71 mmol/g) with standard Fmoc-strategy. Side chain protecting groups were the following: Arg (Pbf), Lys (Boc) and Gln (Trt), while the other amino acids were unprotected. All amino acids were coupled by DIC (N, N′-Diisopropylcarbodiimide)/HOBt (Hydroxybenzotriazole) agents in DMF (Dimethylformamide) with a threefold excess of reagents. After 3 h of coupling, Fmoc-deprotection was performed by piperidine/DMF, 1:4 (*V*/V) mixture for 5 min then repeated for 25 min. After the last deprotection step, a mixture of 93% TFA (trifluoroacetic acid), 2.5% H_2O, 2.5% TIS (triisopropylsilane), 2% DTT (dithiothreitol) was applied for the cleavage during 3 h at 0 °C. After the removal of TFA, crude peptides were precipitated with diethyl ether, dissolved in 50% aqueous acetic acid and lyophilized.

Purification of crude peptides was carried out using a Phenomenex Jupiter C18 column with a gradient of H2O:ACN 100:0 *v*/v to H2O:ACN 50:50 in the presence of 0.1% TFA at a flow rate of 0.5%/min. Analytical HPLC measurements of the purified peptides were performed with a

Table 1
Antibacterial activity of peptides 1–9.

Peptides	MIC[a]/MBC[b] (μg/ml) ($n = 3$)							
	MSSA	MRSA	EC.	LM1-EC	LM2-EC	PI-YE.	MI-SE	LM-S. *sp*
1RQWRRWWQR-NH_2 (+4)	**50/>50**	**25/50**	**25/50**	**12.5/25**	**12.5/50**	**25/50**	**12.5/25**	**25/50**
2 RKFRRKFKK-NH_2 (+7)	>50	>50	>50	>50	>50	>50	>50	>50
3 RQIRRWWM(*O*)R-NH_2 (+4)	**50/50**	**50/50**	**25/50**	**6.25/25**	**12.5/25**	**12.5/25**	**12.5/25**	**12.5/25**
4 RKIRRKWKR-NH_2 (+7)	>50	>50	>50	>50	>50	>50	>50	>50
5 RKIKKRRKKWR-NH_2 (+9)	>50	>50	>50	>50	>50	50	>50	>50
6 RQIKIRRMKWR-NH_2 (+6)	>50	>50	>50	>50	>50	50	>50	>50
7 RWKMRRIKIQR-NH_2 (+6)	>50	>50	>50	>50	>50	50	>50	>50
8 RQPRRWPM(*O*)R-NH_2 (+4)	>50	>50	>50	>50	>50	50	>50	>50
9 RQPKIPRMPWR-NH_2 (+4)	>50	>50	>50	>50	>50	50	>50	>50
Cefotaxime	0.5	0.5	0.5	5	0.5	0.5	12.5	0.5

MSSA: methicillin-sensitive *Staphylococcus aureus*; MRSA: methicillin-resistant *Staphylococcus aureus*; ATCC 43300; EC: *Escherichia coli* ATCC 25922; LM1-EC: LM1-*Escherichia coli*; LM2-EC: LM2-*Escherichia coli*; PI-YE: PI-*Yersinia enterocolítica*; MI-SE.: MI-*Salmonella enteritidis*; LM -S. *sp*.: *Salmonella* sp.; Cefotaxime: positive control. The net atomic charge of each peptide is shown in brackets. M(O): methionine sulfoxide.

[a] MIC: minimal inhibitory concentration.

[b] MBC: minimal bactericidal concentration.

Phenomenex Jupiter C18, column, using different gradient elution protocols, with a mobile phase 80% acetonitrile, 0.1% TFA, at a flow rate 1.2 ml/min.

2.2. Antibacterial activity

2.2.1. Microorganisms and media

The strains from the American Type Culture Collection (ATCC), Laboratorio de Microbiología (LM), Facultad de Ciencias Médicas, Universidad Nacional de Cuyo, Mendoza, Pasteur (PI) and Malbrán Institutes (MI), Argentina were used: methicillin-sensitive *Staphylococcus aureus* ATCC 29213 (MSSA), methicillin-resistant *Staphylococcus aureus* ATCC 43300 (MRSA), *Escherichia coli* ATCC 25922 (EC), LM1-*E. coli* (LM1-EC), LM2-*E. coli* (LM1-EC), PI-Yersinia enterocolitica (PI-YE), MI-Salmonella enteritidis (MI-SE) and LM-Salmonella sp.(LM-Ssp). Each strain was cultivated overnight in Müeller-Hinton broth. To obtain the inocula, adjusted to 1–5 × 105 CFU/ml (colony forming units), we used the guidelines of the Clinical and Laboratory Standards Institute [40].

2.2.2. Antibacterial susceptibility testing

Minimal Inhibitory Concentration (MIC) to the peptides was determined by broth microdilution technique [40]. Stock solutions in DMSO of each peptide were prepared and diluted to give serial twofold dilutions that were added to each medium to obtain final concentrations ranging from 1.56 to 50 μg/ml. The final concentration of DMSO in the assay did not exceed 1%. Antimicrobial agent Cefotaxime® (Argentia Pharmaceutica) was included in the assays as a positive control. The plates (96 wells) were incubated for 24 h at 37° and the effect was evaluated with a spectrophotometer at 620 nm (Multiskan FC instrument).

The Minimum Bactericidal Concentration (MBC) test was performed via inoculation of MIC broth (5 μL) on culture plates containing nutrient agar. The MIC and MBC values were defined as the lowest peptide concentrations showing no bacterial growth after the incubation time. Tests were carried out by triplicate. MIC and MBC values were expressed in μg/ml.

2.3. Liposome preparation

1,2-dioleoyl-sn-glycero-3-phosphocholine (DOPC) and 1,2-dioleoyl-sn-glycero-3-[phosphorac-(1-glycerol)] (DOPG) were purchased from Avanti Polar Lipids Inc. and NOF Europe GmbH.

Liposomes of DOPC and DOPC/DOPG (80:20, n/n%) were prepared by lipid thin-film hydration technique. The required amount of lipids was first dissolved in a chloroform (LabScan, Hungary)/methanol (Reanal, Hungary, 50 vol%) solution, and subsequently evaporated using a rotary evaporator. The resulting lipid film was kept under vacuum overnight to ensure the evaporation of residual traces of solvent and then hydrated with a 10 mM, pH = 7.4 phosphate buffered saline solution (PBS, Sigma-Aldrich, Hungary) to prepare a 13 mM vesicle suspension. After freeze-thaw cycles (at least 10 cycles) using liquid nitrogen and a warm water bath (~40 °C), the sample was extruded (for at least 11 times) through 200-nm polycarbonate filters (Nuclepore, Whatman Inc.) with a LIPEX extruder (Northem Lipids, Inc., Canada).

2.4. Circular dichroism (CD) spectroscopy

CD measurements were conducted using a JASCO J-715 spectropolarimeter at 25 ± 0.2 °C and a 0.1 cm path length rectangular quartz cuvette (Hellma, USA). Temperature was controlled by a Peltier thermostat. CD data were collected by a continuous scanning mode between 190 and 270 nm for the peptides in buffer and between 199 and 270 nm in the presence of liposomes, at a rate of 100 nm/ min, with a step size of 0.1 nm, response time of 4 s, four accumulations, and 1 nm bandwidth. The obtained CD curves were corrected by the spectral contribution of the blank buffer solution. For the measurements, samples were dissolved in 10 mM, pH 7 phosphate buffer. Note that for samples containing liposomes and/or higher aggregates, signals at low wavelengths are not reliable due to light scattering, thus these regions were truncated in the corresponding figures.

2.5. Dynamic light scattering (DLS)

The measurement of the average size and size distribution of liposomes was performed at 20 °C using a W130i dynamic light scattering device (DLS, Avid Nano Ltd., High Wycombe, UK) provided by a diode laser (660 nm) and a photodiode detector. A 80 μL sample was dissolved in PBS and measured in a disposable low-volume cuvette with 1 cm pathlength (UVette, Eppendorf Austria GmbH). The time-dependent autocorrelation functions were obtained measuring the samples 10 times (each measurement for 10 s) and were analyzed with the iSize 3.0 software, supplied with the device.

2.6. Attenuated total reflection Fourier-transform infrared spectroscopy (ATR-FTIR)

ATR-IR measurements were performed with a Varian 2000 FTIR Scimitar Series spectrometer (Varian Inc., USA) equipped with a liquid nitrogen cooled mercury-cadmium-telluride (MCT) detector and a 'Golden Gate' single reflection diamond ATR accessory (Specac Ltd., UK). A 5 μL sample dissolved in PBS was mounted onto the ATR crystal and spectra were collected from the dry film obtained by slow evaporation of the buffer under ambient conditions. For the measurements, 64 scans were co-added at a nominal resolution of 2 cm^{-1}. After each measurement, ATR correction was performed. Spectral analysis was performed using Origin software package (OriginLab, Northampton, MA, USA). Spectra were smoothed applying the Savitzky-Golay algorithm. Buffer subtraction and baseline correction were also performed. Peak positions were determined from the second derivative spectra. For the second derivative analysis spectra were normalized by the area.

2.7. Fluorescence spectroscopy

Spectra were collected using a Jobin Yvon Fluoromax-3 spectrofluorimeter at 25 °C in PBS. Spectra were recorded three times, averaged, and corrected by subtracting a matching blank. For measuring the intrinsic fluorescence of the peptides, fluorophore Trp was excited at 280 nm and its emission was monitored from 300 to 400 nm. Peptides alone were tested at 2.5 μM, 5 μM and 7.5 μM, upon consecutive addition from the stock solution (1 mM in water). Probing liposome binding of the peptides, the same setup was used in the presence of 100 μM PC or PC/PG.

2.8. Flow-linear dichroism spectroscopy (flow-LD)

LD spectra were recorded using a JASCO-1500 spectrometer equipped with a Couette flow cell system (CFC-573 Couette cell holder). The spectra were collected between 190 and 300 nm in 1 nm increments at a scan speed of 50 nm/min with a total path length of 0.5 mm. The samples were oriented under a shear gradient of 2270 s^{-1}. Baselines at zero shear gradients were measured and subtracted. Samples containing 60 μM peptides and 800 μM liposomes were measured in 10 mM sodium phosphate buffer (pH 7.0) containing 45% sucrose. Sucrose can reduce the light scattering of liposomes by matching their refractive index [41].

2.9. TEM experiments

A 2 μL sample containing 2.54 mM lipid and 195 μM peptide, respectively, in PBS, was placed onto a golden sample holder, frozen in liquid Freon at −194 °C and stored in liquid nitrogen. A Balzers freeze fracture device (Balzers BAF 400D, Balzers AG, Liechtenstein) was used to fracture the samples at −100 °C. From the fractured surfaces, replicas

were obtained by carbon-platinum shadowing followed by washing with surfactant solution and distilled water. The replica was transferred to a 200 mesh copper grid and subjected to TEM imaging.

TEM images were taken on a JEOL JEM-1400 transmission electron microscope (JEOL Ltd., Japan) operating at 120 kV. Images were captured routinely at magnifications of x 15,000, x 30,000, and x 60,000, and analyzed with a SightX Viewer Software (EM-15300SXV Image Edit Software, JEOL Ltd., Tokyo, Japan).

2.10. Molecular simulations

In order to compare the results obtained in these simulations with those previously reported for peptides 1 and 2, all simulations were carried out using the same steps and applying the same techniques as used in references [39] and [42]. A brief description of the methodology is presented below as well as in Section 3.3 However, a more detailed description can be obtained the aforementioned references.

2.10.1. Cell membrane model for simulations

A zwitterionic phospholipid bilayer of DPPC composed of 648 DPPC molecules (324 per leaflet) and 28,526 water molecules of the single point charge (SPC) [43] was considered the cell membrane model in our simulations. The reason for choosing a zwitterionic bilayer for the simulations is based on the results previously obtained for the dynamics action mechanism [39]. This study demonstrated how small cationic peptides induce phospholipid segregations of lipid domains prior to showing lytic activity, when they reach a threshold concentration on the surface of the cell membrane and then penetrate into the membrane of the domains that are rich in zwitterionic phospholipids.

2.10.2. MD simulations

GROMACS 4.5.3 [44,45] was the package used to carry out the MD simulations. All simulations were performed in NPT conditions, using the algorithm proposed by Berendsen [46] with coupling constants of 0.1 and 1 ps for temperature and pressure, respectively. The simulation temperature was 350 K, which is above the transition temperature of 314 K of DPPC bilayers [47]. Long-range interactions were simulated using the Lennard-Jones potential, and the electrostatic interactions were calculated using the particle Mesh Ewald method [48,49] with a cut-off 1 nm. Molecular bonds were restrained using LINCS algorithm [50]. The SPC water model [43] was considered in all our simulations. A trajectory length of 200 ns was simulated in all the cases studied here. The force field used in this study was the same as described previously [39] using the GROMOS 54A7 force field [51] implemented in the GROMACS package.

3. Results and discussion

3.1. Design strategy, synthesis, and antibacterial activity of new short cationic antibacterial peptides

The main objective of this work is to understand the mechanism of action of these short-sized antibacterial cationic peptides (SACP). The peptides studied in this work have been designed in order to evaluate different structural properties such as charge, secondary structure, hydrophobicity and amphipathic characteristics that allow us to further understand the interactions with their target (i.e. biomembranes). When designing the modifications, we only considered the sequence of the peptides. Hence, the size and type of sequence of the peptide was taken into account as well as how the replacement of different amino acids could alter the biological effect of each compound. Table 1 shows the synthesized peptides and details of their synthesis process are described in the methods section.

There are previous reports on attempts to determine the possible mechanism of action of these SACPs by using molecular dynamics simulations [39]. More recently, the influence of charge on the antimicrobial activity of small cationic peptides was evaluated [42]. In this last study, peptide 1 showed a significant antibacterial activity; moreover, this peptide has previously been reported as a potential antifungal agent [24]. However, peptide 2 was found to be inactive against bacteria [42] and fungi [26]. Consequently, in the present study peptide 1 and 2 are ideal as reference sequences in antibacterial activity, and therefore have also been tested under the same conditions as the other peptides in this study (see Table 1).

Some amino acids have been found to increase activity in general; among them Lys, Arg and Trp are the most cited [52–54]. It also has been observed that arginine and lysine substitutions are more effective when complemented with tryptophan (W) because it can act as hydrophobic counterpart, balancing the cationic charge provided by Arg (R) and Lys (K). On the other hand, it is well-known that Pro (P) has the characteristic to alter the secondary structure of peptides. Thus, the structural changes performed in peptides evaluated have been mainly carried out adding or changing the above-mentioned residues.

Peptide 3 is an analogue of 1, in which two amino acids have been replaced, namely Ile (I) by Trp (W) and Met (O) by Gln (Q). As expected, this peptide showed significant antibacterial activity (Table 1). In fact, its activity is very similar to that of peptide 1. It should be noted that peptide 3 has a net charge of +4 and the same number of hydrophobic residues as peptide 1. In general, the MBC values were about 2-fold higher than the final MIC of each active peptide.

Peptides 4–9 are analogues of 3 with different modifications in their sequences. Peptide 4 is an analogue of 3 in which three amino acids (Gln, Trp and Met (O)) have been replaced by lysine residues in order to increase their positive charge increase from +4 to +7, while in Peptide 5 we added two additional Lys (K) residues giving it a +9 charge. We also synthesized peptide 6, which is structurally related to peptides 1 and 3, in which two Lys (K) residues have been added into the central portion of its sequence giving it a charge of +6. It should be noted that peptides 5 and 6 have eleven residues instead of nine as in peptides 1 and 3. These peptides have been designed in order to gradually increase their cationic charge: +6 (peptide 6), +7 (peptide 7) and +9 (peptide 5). In peptide 8, two residues (Ile and Trp) have been replaced by Pro (P), whereas in peptide 9, three Pro residues have been included in its structure. Our main objective when making these changes was to alter the secondary structure of these peptides.

Once we synthesized these peptides, our next step was to evaluate their antibacterial activities. These results are shown in Table 1. Some of the results obtained here were expected, such as the lack of activity of peptide 5 due to its excessive positive charge (+9). Similarly, the lack of activity of peptides 8 and 9 was also somewhat predictable due to the presence of Pro residues affecting their respective secondary structures. However, the lack of activity of peptides 4 (+7), 6 (+6) and 7 (+6) was an unexpected result, because there are many peptides reported as antibacterial compounds that have a net charge +6 or +7. The importance of net charge in the antibacterial activity of these peptides is well-known. However, for these short-sized peptides the load-hydrophobicity ratio as a function of the number of residues seems to be even more delicate than in the case of long-sized peptides. To further understand these results, we carried out more specific structural studies including experimental techniques and molecular simulations, for which the four most characteristic peptides of this series were selected (compounds 1, 2, 5 and 6). It should be noted that for this study we chose an active peptide (compound 1) and three inactive ones (peptides 2, 5 and 6).

3.2. Structure, morphology and membrane affinity of SACPs

3.2.1. Peptide structural changes assessed by circular dichroism spectroscopy

Some active peptides change their secondary structures upon interaction with the lipid bilayer [55]. CD spectroscopy was used to monitor the peptide secondary structure both in buffer solution and in the presence of dioleoylphosphatidylcholine (PC) and

dioleoylphosphatidylglycerol (PG) liposomes, as simple models of mammalian and bacterial membranes, respectively. As mentioned above, selected peptides 1, 2, 5 and 6 can be considered the most representative of the series, according to their number of residues, charge and biological activity. The 9-mer peptides 1 (+4) and 2 (+7) are regarded as references for active and inactive peptides, respectively. The 11-mer peptide 5 is characterized by its highest positive charge (+9) which could be the cause of the expected lack of antimicrobial effect. On the other hand, peptide 6 (+6) resulted surprisingly inactive, even though it is structurally closely related to peptides 1 and 3. The CD spectra of peptides 1, 2, 5 and 6 are shown in Fig. 1a–d. Peptide 1 has distinctive spectral features compared to the other studied peptides. The CD spectrum of peptide 1 (Fig. 1a) dissolved in buffer is constituted by two negative bands with a minima located near 200 nm and 225 nm and a maxima around 215 nm. These spectral features have been attributed to the stacking of adjacent Trp residues or their interaction with the peptide backbone [56]. Indeed, aromatic side chain chromophores have non-negligible contributions in the range 180–230 nm due to the intense π-π* transitions and their closer vicinity to the peptide backbone compared to other amino acids. This strong contribution from the aromatic side chains impeded the estimation of the peptide's secondary structure and only qualitative information could be deducted. CD spectra showing this spectral profile have been interpreted as β-turn structures in Trp-rich peptides which, however, also contain proline residues that are more likely to fold [57–59]. CD spectra of the investigated peptides were also recorded in the presence of liposomes. To retain a consistent peptide to lipid ratio for all methods employed, to maximise spectral intensities and to simultaneously avoid high light scattering due to liposomes, the peptide to lipid ratio of 1:13 was determined as a compromise and used throughout the study unless noted otherwise. The spectrum obtained for peptide 1 after adding neutral PC vesicles is slightly shifted to lower values, probably indicating weak electrostatic interactions with the zwitterionic lipid bilayer. Note that different spectral variations were observed upon addition of PC/PG liposomes. In this case, the significant decrease in intensity of the minima at ~226 and ~199nm and the increase of the maxima at ~212 nm, which also slightly shifted downwards, is suggesting a stronger interaction with the negatively charged membrane and possible aggregation (Fig. 1a). In this case, structural variations could be determined by electrostatic attractions between the basic residues and the negatively charged PG head groups, together with hydrophobic interactions between the aromatic side chains and the bilayer non-polar central portion [60].

The CD spectra for peptides 2, 5 and 6 displayed a similar spectral profile characterized by a single negative band around 197–200 nm, which is characteristic in disordered peptides [61] (see Fig. 1b–d). Peptide 2 is also characterized by a positive band at ~220 nm that could be due to the aromatic Phe side chains [62] and is slightly shifted to lower values in the presence of PC/PG (Fig. 1b). In contrast to peptide 1, peptides 2, 5 and 6 did not show significant variations in the presence of lipid membranes compared to the buffer solution. However, in the case of peptide 5 the spectral intensity slightly reduced with the addition of PC/PG, probably suggesting moderate aggregation (Fig. 1d).

Results from CD investigations revealed remarkable spectral changes for peptide 1 in the presence of lipid membranes, especially for the negatively charged PC/PG vesicles. Conversely, spectral profile of peptides 2, 5 and 6 did not experience significant variations in the presence of lipid vesicles, although minor changes were observed for peptides 2 and 5 upon addition of negatively charged membranes. It is noteworthy that peptide 1 is the only tested compound active against several bacterial strains (Table 1), most likely due to its peculiar ability to interact with negatively charged membranes, as suggested by CD investigations.

3.2.2. *Peptide-induced liposome aggregation*

The aggregation propensity observed for peptide 1 and, to a lesser extent, for peptide 5 (Fig. 1a and c) was also monitored by DLS

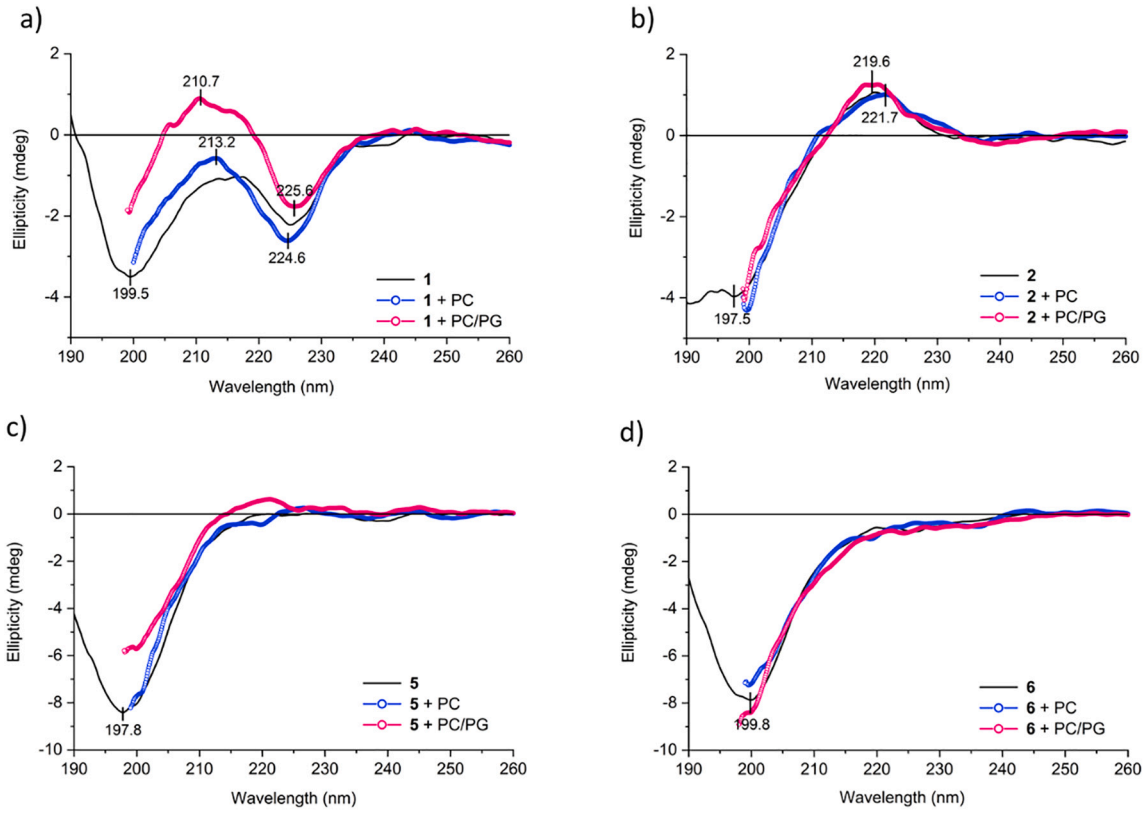

Fig. 1. Far-UV CD spectra of the peptides in buffer and following the addition of PC and PC/PG (8:2) liposomes. Peptide concentration is 60 μM and peptide-to-lipid ratio is 1:13.

measurements. In the case of neutral PC vesicles (Fig. 2a), the correlation functions were comparable for all the studied peptides and indicated an average diameter of ~160 nm, the size of the liposome. Conversely, a significant shift toward higher decay times can be observed for PC/PG vesicles in the presence of peptides 1 and 5 (Fig. 2b), indicating the formation of larger assemblies. Indeed, hydrodynamic diameter values in the low-micrometer range were calculated for peptides 1 and 5 (Table 1 SI). Based on the calculated size distribution, however, the peptide-induced-effect on liposome size is the most pronounced for peptide 1. Thereby, DLS results support the formation of molecular aggregates upon interaction of peptide 5 and particularly for peptide 1 with negatively charged membranes. To further investigate the effect of the peptides on liposome size and integrity, we utilized TEM, which provides information about the morphology of particles, too. In contrast to vesicle control where only isolated liposomes were observed (Fig. 2c), bigger vesicle-agglomerates could be imaged for each peptide-PC/PG mixture (Fig. 2c, peptide 1 is taken as a reference), although to a different extent. Based on thorough visual inspection, the tendency to induce liposome aggregation was as follows: peptide 5 > peptide 1 ~ peptide 6 >> peptide 2. For peptide 2, intact liposomes dominated and only a few aggregated clusters were detected. To compare, the reference peptide 1 was also tested with PC vesicles. In this case, higher sized agglomerates were not found, but the peptide could connect a few bilayers. This is in line with the ability of peptide 1 to perturb neutral membranes as indicated by IR data, although through a mechanism other than the effect exerted on anionic bilayers.

3.2.3. *Peptide-vesicle interactions studied by infrared spectroscopy*

The secondary structure of the investigated peptides and their mechanism of interaction with lipid membranes have been further analyzed by means of ATR-IR spectroscopy (Fig. 3). The infrared signal is, indeed, not affected by aggregation and the presence of aromatic side chains, permitting the study of the peptide structure together with interactions involving the polar and apolar moieties of lipid membranes. The amide I region profile of the peptides in buffer (Fig. 3a) denoted, in general, the prevalence of turns (1668 cm^{-1}, 1675 cm^{-1}) and random coils (1647 cm^{-1}), while small contributions from inter-molecular interactions and oligomerization (1616 cm^{-1}, 1627 cm^{-1}) can be observed for peptides 5 and 6. In the presence of zwitterionic PC liposomes the amide I of peptides 2, 5 and 6 shifted toward higher wavenumbers with the main contribution at 1683 cm^{-1} (Fig. 3b, left panel). This latter can be commonly assigned to turns, aggregated strands/intra-molecular β-sheets [63,64] and but it has also been attributed to peptide extended conformations located at the membrane surface [65]. In addition, peptide 5 and 6 exhibited a less intense shoulder at 1625 cm^{-1}. Among the studied compounds, the spectral profile of peptide 1 differed from the others, showing a more intense peak at 1676 cm^{-1} and a shoulder at 1628 cm^{-1} (Fig. 3b, left panel), which are consistent with unordered conformations and aggregation of the peptide chains [66–68] respectively. In the presence of PC/PG negatively charged membranes (Fig. 3b, right panel), it is possible to observe modest shifts of the peaks at 1676 and 1683 cm^{-1}, especially in the case of peptide 1. For this latter, the increased intensity of the shoulder at ~1626 cm^{-1} suggests more extensive aggregation in the presence of negatively charged membranes. In order to better quantify aggregate formation study spectral alterations related to the formation of aggregates compared to other structures, peptide spectra were curve fitted in the region 1800–1460 cm^{-1} and the area ratio of the two main spectral components located at ~1625 cm^{-1} (aggregates) and ~1675 cm^{-1} (non-associated random coils and turns) calculated and displayed in Fig. 1a SI. Notably, in the case of peptide 1 results indicated approximately a three-fold increase of aggregated over non-aggregated mainly disordered

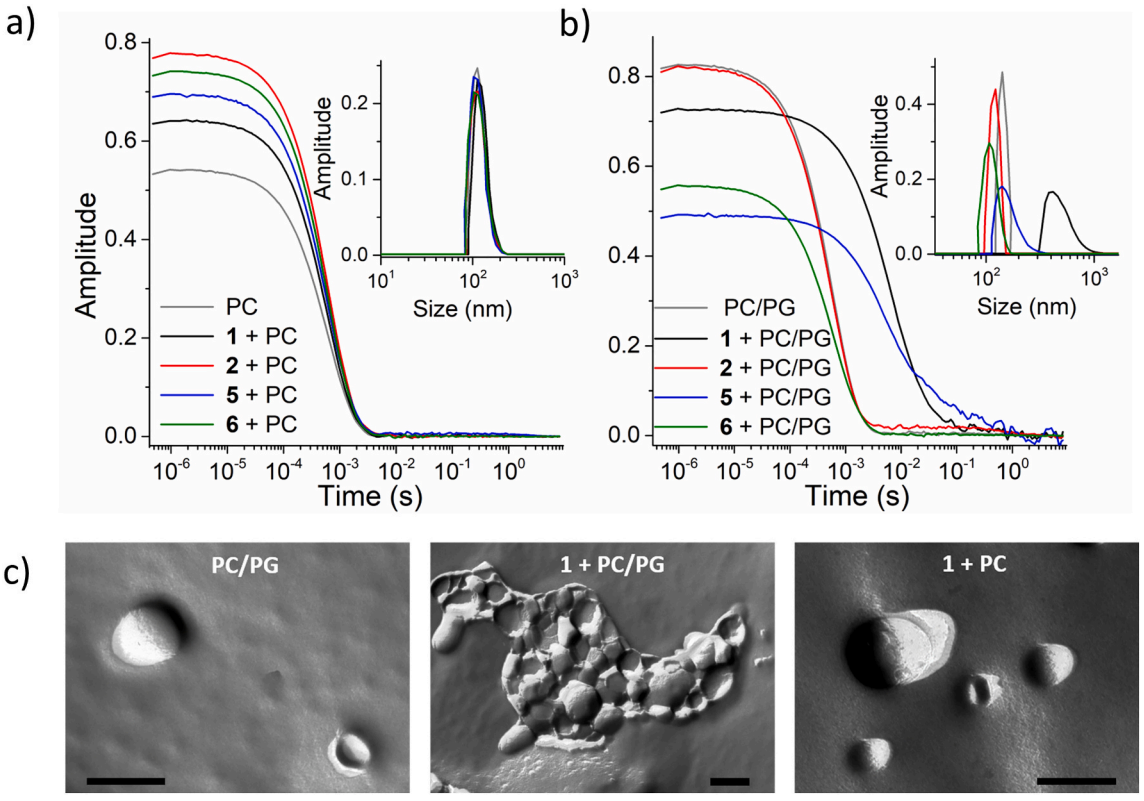

Fig. 2. Influence of the peptides on the liposome size and morphology monitored by DLS and FF-TEM. Correlation functions of PC (a) and PC/PG (8:2) (b) liposomes alone and in the presence of the studied peptides. Insets show calculated size distributions. Peptide concentration is 50 μM and peptide-to-lipid ratio is 1:13. c) FF-TEM pictures of 200 nm PC/PG (8:2) and PC liposomes in the presence of peptide 1. Peptide concentration is 195.4 μM and peptide-to-lipid ratio is 1:13. Scale bars: 200 nm.

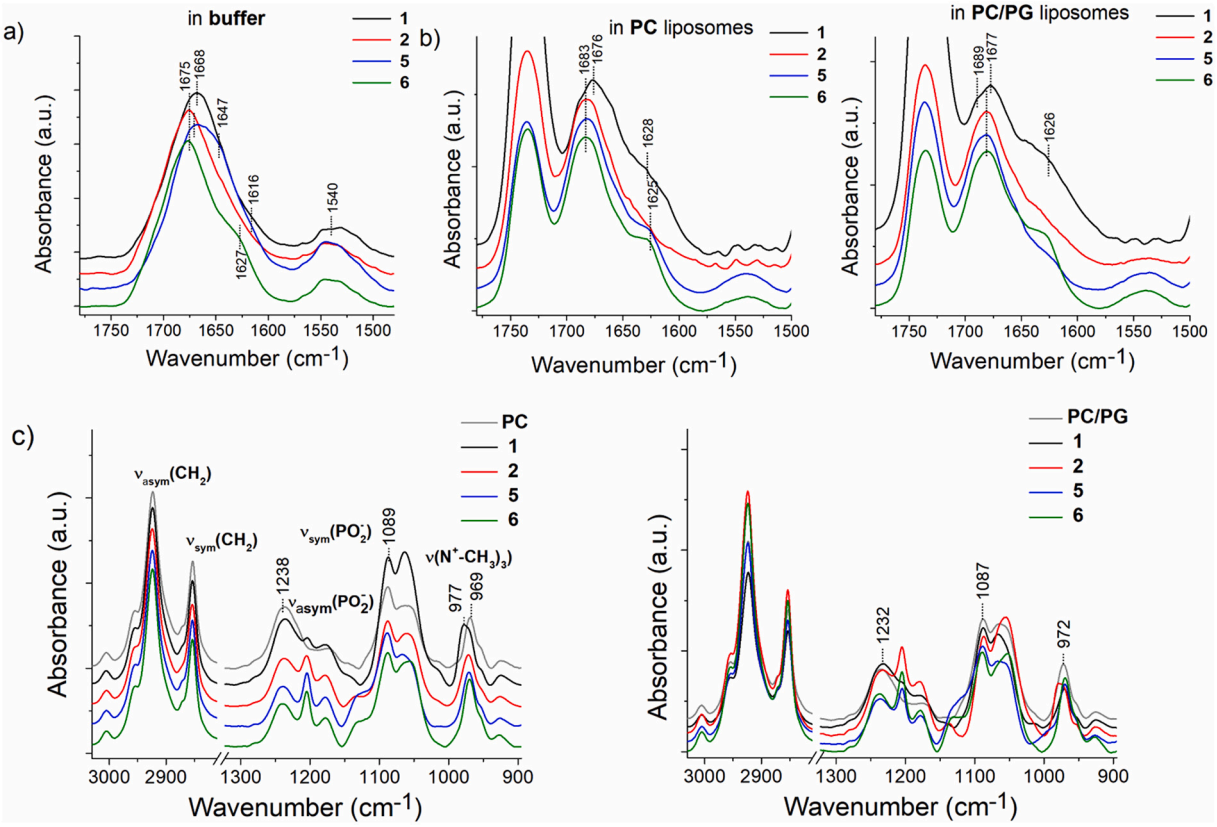

Fig. 3. ATR-IR study of the peptides in buffer solution and in the presence of membrane model systems. Amide *I* and II region of the peptides in buffer (a) and in PC or PC/PG liposomes (b). Spectra are normalized by the intensity of the amide I peak. Peak position was determined by second derivative analysis. c) Acyl chain ($\nu_{sym}(CH_2)$, $\nu_{asym}(CH_2)$) and head-group region ($\nu_{asym}PO_2^-$, $\nu_{sym}PO_2^-$, $\nu(N^+\text{-}(CH_3)_3)$ of PC (left panel) and PC/PG (right panel) membranes alone and in the presence of the analyzed peptides. Spectra are normalized due to the intensity at 2920 cm^{-1} (in the high-frequency region) and at ~1090 cm^{-1} (in the low-frequency region). Peptide concentration is 160 μM and peptide-to-lipid ratio is 1:13.

structures upon interaction with PC/PG liposomes. For the other peptides, variations of the 1625/1675 cm^{-1} ratio were less pronounced, however, higher values can be observed in the presence of PC liposomes.

The analysis of the amide I band revealed that the structure of the studied peptides is mostly unordered in buffer while in the presence of lipid membranes the contribution from aggregated conformations becomes more prominent, especially upon interaction of peptide 1 with negatively charged membranes. Notably, peptide 1 exhibited peculiar features, suggesting a different mechanism of interaction compared to the other studied peptides.

The interaction between the studied peptides and lipid membranes was further explored by analysing the vibrational modes in the infrared spectral regions that are characteristic for phospholipid molecules (Fig. 3c). Results show that the methylene stretching of acyl chains ($\nu_{sym}(CH_2)$ and $\nu_{asym}(CH_2)$) was not affected by the presence of the peptides in both lipid systems (Fig. 3c). On the contrary, relevant spectral modifications can be observed in the polar head group region (1300–900 cm^{-1}), suggesting potential interactions with the membrane surface. In the case of PC liposomes, it is worth noting that only the addition of peptide 1 caused a red shift of the phosphate asymmetric and symmetric stretching ($\nu_{asym}PO_2^-$, $\nu_{sym}PO_2^-$) (Fig. 3c, left panel), denoting more established interactions with phosphate groups. The interaction of peptide 1 with phosphate groups is reflected in the alteration of the environment around the choline group, as suggested by the shift of the $\nu(N^+\text{-}(CH_3)_3)$ band. Moreover, variations in the relative intensity of the shoulder at ~1060 cm^{-1} (R-O-P-O-R' stretching of phosphate diester) indicate an altered internal packing of lipid head groups upon the addition of all the studied peptides. More complex spectral modifications can be observed for PC/PG membranes, where all the peptides altered the spectral profile of the phosphate groups. A particularly remarkable alteration is the red shift of $\nu_{asym}PO_2^-$ caused by peptides 1 and 2, whereas peptides 5 and 6 induced a shift of $\nu_{asym}PO_2^-$ in the opposite direction. Additionally, analysis of the carbonyl band (Fig. 1 SI) revealed a small red shift in the presence of peptide 6, suggesting a moderate interaction with the lipid polar/non-polar interface.

It has been shown that the mechanism of action of small cationic peptides and their toxicity toward bacterial cells considerably depends on their concentration [39,69]. Higher lipid content can affect the peptide secondary structure and, consequently, its interaction with the membranes. Since intensities arising from the peptide in the IR spectra were sufficiently high, here we also employed measurements where the lipid-to-peptide ratio was changed to 65:1. By increasing the lipid-to-peptide ratio (Figs. 2–3 SI), the amide I band of all the investigated peptides showed an additional component at ~1655 cm^{-1} (Figs. 2–3a SI), commonly assigned to α-helical structures [70]. Moreover, the phospholipid head groups were less affected by the presence of the peptides and only moderate variations were induced by peptide 5 and 6. Nevertheless, these have not resulted in drastic changes in the observed spectra.

In summary, IR investigation revealed that the studied peptides preferentially interact with the membrane surface, rather than the centre of the lipid bilayer. Indeed, all peptides perturbed the membrane hydrophilic region, especially the negatively charged PC/PG membranes, but only peptide 1 showed an interaction with the phosphate groups of both PC and PC/PG vesicles. Furthermore, the increase of the lipid content affected peptide structure, and the effect on membrane polar head-groups was subsequently reduced considerably.

3.2.4. Lipid partition of tryptophan-containing peptides detected via intrinsic peptide fluorescence

In order to explore additional peptide interactions with lipid bilayers, peptide intrinsic fluorescence was monitored for peptides 1, 5, and 6, containing Trp residues. Trp fluorescence is a useful tool to probe the polarity of the Trp microenvironment, which can change upon peptide interactions [71]. In the absence of model membranes, an emission maximum of ~357 nm (Fig. 4 and Fig. 3 SI) indicated fully water accessible Trp side chains of a presumably unordered conformation in all three peptides at each concentration studied. A threefold higher intensity measured for peptide 1 compared to peptides 5 and 6 is consistent with the presence of three Trp residues in the former compared to the one only Trp in the latter two peptides. Upon the addition of neutral PC liposomes, no change in the emission signal was detected for any of the peptides compared to the lipid-free state, suggesting the absence of any significant interaction between the peptides and the zwitterionic lipids, at least regarding the detectable partition of the Trp side chains. In contrast, a blue shift of the emission maximum, concomitant with an enhancement of the intensity, was observed when negatively charged PC/PG liposomes were added (Fig. 4b, d and Fig. 4b SI). The effect was most remarkable with peptide 1, considerably present for peptide 5 and less pronounced for peptide 6. To address the effect of peptide to lipid ratio, beside 1:13, we have also investigated 1:20 and 1:50 ratios, while keeping the lipid concentration constant (Fig. 4). Moreover, the extent of the blue shift was shown to depend on the peptide-to-lipid ratio as the highest shift was observed in the case of the lowest peptide concentration applied. This indicated that a less crowded condition allows a binding mode where the Trp indole rings can be more separated from the solvent. However, the position of even the most significantly shifted maximum, 347 nm for peptide 1 at the highest lipid-to-peptide ratio, is indicative of partially water-exposed Trp residues. These findings are consistent with peptide binding to PG lipids resulting in a more hydrophobic Trp environment of a partially buried Trp side chain localized near the bilayer surface rather than fully inserted into the membrane. Note, that the highest effect observed for peptide 1 over peptides 5 and 6 is in agreement with their antibacterial efficacy (Table 1) and suggests a mechanism for peptide 1 where the biological effect is linked to its membrane association ability.

3.2.5. Orientation of liposome-bound peptides suggested by flow-LD spectroscopy

Changes induced on the model membrane systems by peptides were also investigated by linear dichroism spectroscopy. LD is defined as the difference in absorption of linearly polarized light oriented parallel and perpendicular to a macroscopic orientation axis (Eq. (1)).

$$LD = A - A \quad (1)$$

Coupled to a Couette flow cell, where shear force can be created, the lipid vesicles can be distorted from spherical shape to a more ellipsoid prolate spheroid [72].

As a consequence, the lipid bilayer phase will be oriented and thus LD can give both qualitative and quantitative information about membrane insertion and orientation angles of the associated molecules [73–76]. Moreover, the LD signal depends on the secondary structure of the peptide, and while the signal is very informative for e.g. α-helix, in contrast for peptides with unordered structure no LD signal is observed. To monitor the orientation of peptides on or in the membrane we have focused mainly on the tryptophan side chain orientation. The indole ring of tryptophan has three main transition moments, one at 225 nm corresponding to the Bb absorption; the broad La band with maxima ~270 nm and the Lb absorption band with two peaks at 290 nm (see Fig. 5).

The LD spectrum of peptide 1 in the presence of PC liposomes (Fig. 5) exhibited a positive band of peptide bond π-π* origin at ~210 nm, a negative peak at 225 nm corresponding to tryptophan Bb and n-π* transitions of each peptide bonds, where the latter one being much

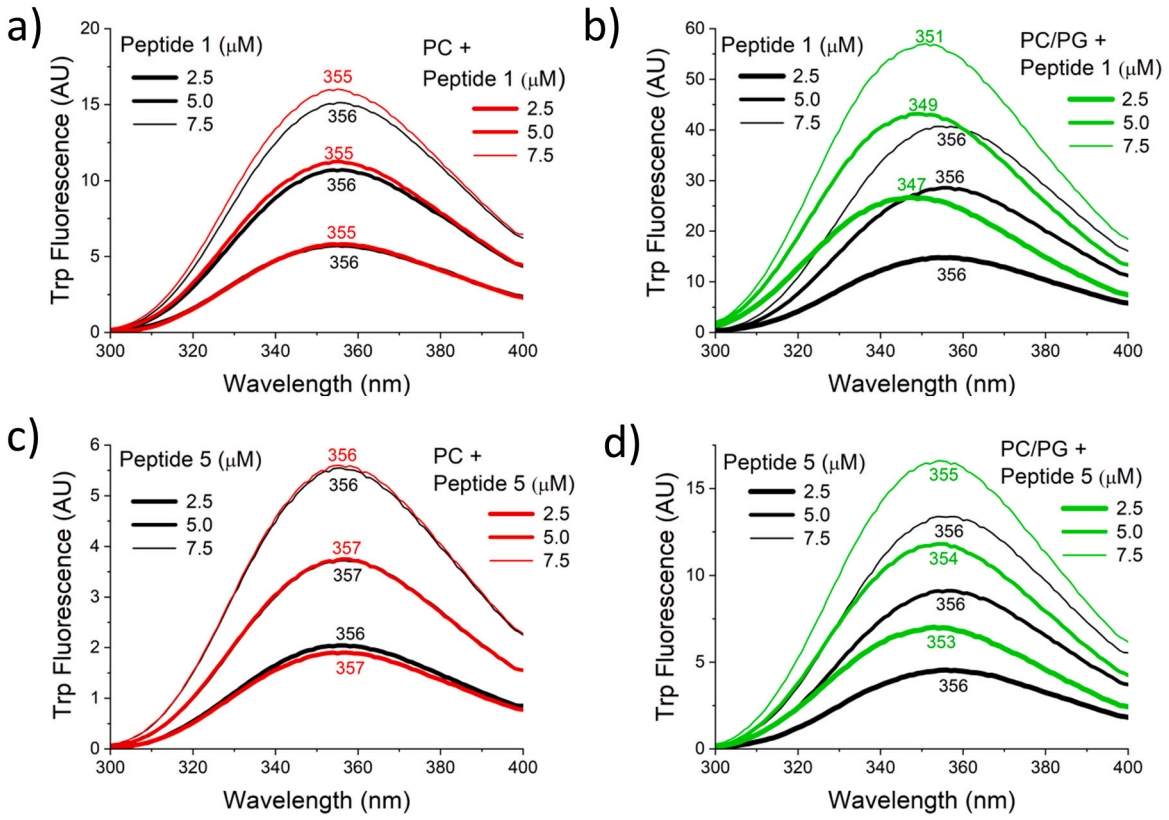

Fig. 4. Fluorescence spectra of the peptides in the presence and absence of PC and PC/PG liposomes. The position of the emission maximum is also indicated for each spectrum. Lipid concentration was 100 μM.

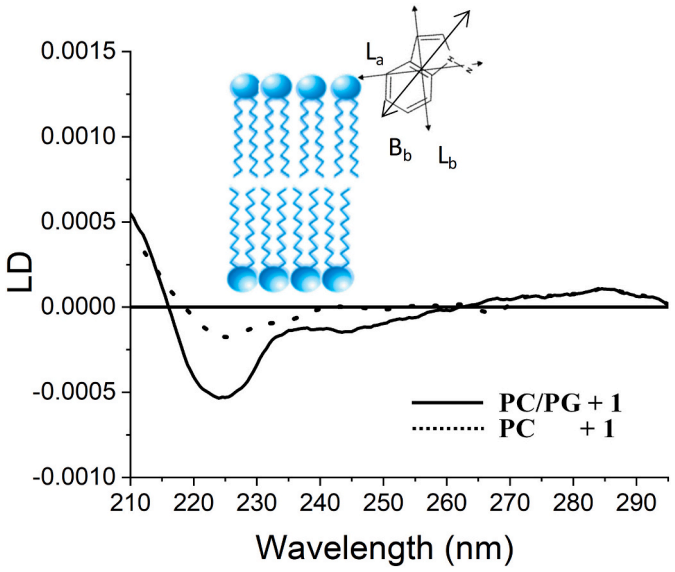

Fig. 5. LD spectra of the peptide 1 in the presence of PC and PC/PG liposomes. Schematic illustration of the average orientation of Trp relative to the lipid bilayer. The electronic transition moment directions in the indole chromophore of tryptophan are also depicted and described in the text. Peptide concentration is 80 μM and peptide-to-lipid ratio is 1:13.

weaker than the Bb transitions. Considering that there are only a few peptide bonds present together with three tryptophans and while normally this spectral region reflects to peptide or protein secondary structure, in the current case it is dominated by the contribution from the Trp transition moments similarly to the case of gramicidin [77]. In addition, two weak, positive peaks around 270 and 290 nm were detected, similar as for penetratin derivatives which indicate an average orientation of the indole plane parallel to the membrane surface [78,79]. Upon addition of peptide 1 to PC/PG liposomes, a significant enhancement in peak intensities was observed (Fig. 5). These suggest a stronger interaction with the negatively charged lipid components driven by electrostatics and also show a preferentially more perpendicular orientation of the Bb transition in the indole chromophore of Trp relative to membrane surface. In contrast, for peptides 2, 5 and 6 in the presence of PC or PC/PG liposomes very weak LD signals were detected (Fig. 5 SI), which is in line with expectations based on CD and fluorescence measurements (Fig. 4a and b, SI). The only exception to be noted is peptide 6, where in the presence of PC/PG a similar, though lower intensity, LD spectrum occurs as for peptide 1, indicating that the single Trp in 6 has a side chain orientation comparable to those of peptide 1.

In summary, the highest spectral contribution of the peptide 1 is in line with observations by IR and fluorescence spectroscopy and the LD signal suggest that the three tryptophans have an anchoring role in fixing the peptide on the surface of PC/PG bilayers.

3.3. Molecular dynamics simulations

Molecular dynamics (MD) simulations have been accepted as a valuable complementary tool in experimental studies to understand complex systems. In our study, Gromacs package 4.5.3 [44,45] was used to carried out our simulations. A time step of 2 fs was used in all simulations. Long range interactions were simulated using the Lennard Jones potential, and electrostatic interactions were calculated using the Particle Mesh Ewald method [48,49], with a cut-off of 1 nm. Molecular bonds were restrained using the Lincs algorithm [50] and simulations were carried out under NPT thermodynamic conditions, with a weak temperature and pressure coupling bath algorithm [46] to the temperature and pressure of 310 K and 1 atm, with coupling constants of 0.1 and 1 ps for temperature and pressure, respectively. Under these conditions, 100 ns of trajectory length were simulated for different numbers of peptides adsorbed on the surface of the lipid bilayer. All simulations were carried out at 350 K, a temperature chosen because it is above the transition temperature of 314 K [47] for pure bilayers of DPPC.

Bilayers of different DPPC were simulated using the force field described in previous studies [80], and the peptide was simulated using the GROMOS 54a7 forcefield [51]. Finally, the single point charge [43] (SPC) was the water model considered in all our simulations.

In this context, we have recently reported results for peptides 1 (+4) and 2 (+7) using the MD methodology described above [42], and in this study we extended this analyses to peptides 3, 4 and 5, with charges +3, +7 and +9, respectively.

3.3.1. Thermodynamic study of peptide insertion in the lipid bilayer. Free energy associated with peptide insertion into the lipid bilayer

The partition function of a certain species between two mediums is directly related with the difference of free energy associated with this process, as follows:

$$\Delta G(z) = -RT\, In \frac{C(z)}{C^*}$$

where C(z) corresponds to the species concentration at a certain position z perpendicular to the interface and C* its concentration in the bulk solution. For the simulations, we used the same approaches previously reported [39] by using Umbrella [81] and PMF was estimated with WHAM [82] computational tools.

As expected, the results obtained for peptide 3 are very similar to those previously reported for peptide 1. In turn, the results obtained for peptide 4 are very similar to those observed for peptide 2 [42]. For increased simplicity in the discussion, we refer to pep + 4 for the results obtained for peptides 1 and 3, pep + 7 for the results of peptides 2 and 4 and pep +9 for those of peptide 5. Fig. 6 shows ΔG(z) values corresponding to the insertion into the DPPC bilayer of the three type of cationic peptides studied here. Fig. 6 shows how the adsorption of peptides into a lipid bilayer is a spontaneous process for these peptides, which corresponds to the negative values of ΔG(z).

Previous studies allow us to propose a mechanism of action for this type of small-size peptides. Our model for antimicrobial activity depends on a combination between electrostatic peptide-peptide interactions and peptide-membrane interactions. Our simulations show that all the simulated peptides have minor tendency to penetrate the bilayer, where the observed affinity order is peptides 1 and 3 (charge +4) = peptide 5 (charge +9) >> peptides 2 and 4 (charge +7). This indicates that it is

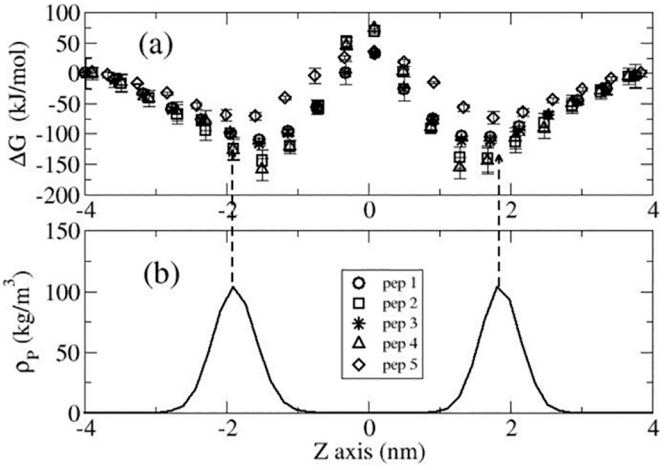

Fig. 6. (a) Free-energy profile associated with the insertion of cationic peptides into a DPPC bilayer. (b) Atomic phosphorous distribution across the DPPC bilayer.

very difficult for a pep + 7 to penetrate the bilayer, and therefore has hardly no tendency to break the lipid bilayer structure. Likewise, it is also very important to consider the proclivity each peptide has of interacting with the surface of the lipid bilayer. In this case, the order of affinity for the surface is the following: pep + 7 > pep + 4 > pep + 9, where the highest affinity is for pep + 7, and the lowest for pep + 9. Thus, these simulations indicate that pep + 7 has the greatest affinity for the surface of the lipid bilayer, but the lowest tendency to penetrate it due to its high peptide-peptide repulsion, and in turn low antibacterial activity is to be expected. Results of our simulations might explain the lack of activity observed for these peptides supporting the experimental studies discussed in the previous sections Peptide 5 has the lowest affinity for the bilayer surface and the highest peptide-peptide repulsion (which prevents reaching a critical concentration of peptide on the bilayer surface). It also shows a low tendency to penetrate the bilayer (similar to peptide 1). Therefore, low antimicrobial activity can also be expected for the peptide 5.

It is interesting to note that peptides 1 and 3 have an intermediate affinity for the membrane surface and a lower charge than pep + 7 and pep + 9, which allows achieving a higher concentration of peptide on the surface of the membrane. Furthermore, peptides 1 and 3 show an acceptable tendency to penetrate the membrane. As a consequence, as peptides 1 and 3 present an intermediate situation between surface affinity, lower peptide-peptide interaction and a higher tendency to insert themselves in the membrane, it is reasonable to expect that they present greater antimicrobial activity, as was observed in the experimental data.

In summary, our simulations suggest that for a small-size peptide to have antibacterial activity it must hold a delicate balance between affinity for the bilayer surface, low peptide-peptide repulsion (in order to reach the threshold concentration) and an acceptable tendency to penetrate the bilayer. Considering the interaction energies and critical density of the peptide on the bilayer surface, it is clear that peptides 1 and 3 are the only ones in this series with the adequate structural characteristics to produce antimicrobial activity.

4. Discussion

As the molecular connections between bacterial membranes and short AMPs are based on nonspecific interactions such as hydrophobicity and electrostatics different sequences and structures can be effective as antimicrobial agents. It seems that the order of amino acids in these short peptides is not always essential for their antibacterial activity. However, the total amount and type of cationic and lipophilic residues seems to be more important, with Arg and Trp being the most relevant of the natural amino acids. For example, the guanidinium group of Arg has a more disperse positive charge than the single amine of Lys which possibly enhances electrostatic interactions between peptides and membrane surface [78,79]. Moreover, the side chain of Arg can interact both electrostatically and by hydrogen bond formation with the negatively charged surface of bacteria membranes rendering a beneficial characteristic to this amino acid. In the case of Trp, its relevance might be attributed to its preference for the water-phospholipid interface region when the peptide is incorporated into membranes [78,79]. Current results from structural investigations on selected peptides also support the important role of tryptophans in anchoring the peptide backbone to the bilayer surface. The size of the aromatic residues is also essential in the disruption of membrane integrity and can explain the increased performance of Trp compared to Tyr. Based on our results, the combination of four Arg and at least two Trp residues (as in peptides 1 and 2) constitutes an efficient motif in short antimicrobial peptides. Our results are fully in agreement with previous works showing that the order of amino acids in short peptides is not as important as the overall composition regarding cationic and lipophilic residues [83,84].

It has been proposed that membrane perturbation by cationic antimicrobial peptides takes place via membrane destabilization or transmembrane pore formation [85]. Considering the short lengths of the peptides reported here, it seems reasonable that these compounds attack bacteria via membrane disruption rather than end-to-end pore assembly as in the case of gramicidins. Our experimental results, as well as the molecular simulations, support this hypothesis. Both the experimental results and molecular simulations seem consistent with an intercalation model [86,87]. In addition to these, our calculations also show that membrane collapse due to the presence of peptides should take place in a relatively small time window. For instance, DLS and TEM images show a morphology with multiple fused vesicles, clearly indicating a strong membrane perturbation by the selected SACPs. On the other hand, both IR spectra and free energy profiles obtained in simulations show that the peptides primarily prefer to reside in the headgroup region, rather than in the acyl chain region of the bilayer. Therefore, intercalation of these short peptides in the membrane could produce an increase in lateral pressure near the interface resulting in a local disruption of the packing of lipid chains. Furthermore, the experiments suggest that the peptides are present in a non-monomeric assembled form that could improve their effect on membrane integrity.

It has been previously shown that there is a concentration dependency for peptides, such as alamethicin, interacting with vesicles [88]. In fact, several articles refer to a threshold concentration for these peptides to have antimicrobial activity [89,90]. Our simulations also indicate the need for this peptide threshold [39]. For peptides as short as peptides 1 and 3, the formation of an intermolecular structure seems to be more favourable than an intra-molecular structure. Therefore, we can speculate that peptide length would provide a greater facility for achieving inter-peptide interactions rather than forming particular internal structure. Additionally, in this process peptide charge seems to play a determining role. It is clear that the peptide must have a positive charge in order to interact with the negative membranes, but this load must not be too great to prevent it from associating with other peptides in order to form the required threshold concentration of peptides. This study shows that for peptides with nine residues a +4 charge is near optimal. This narrow balance between total peptide size, net charge, and hydrophobic characteristics appear to be critical, as our short peptides with +6 or higher charges lose antibacterial activity. It is important to note that these peptides (active and non-active), show different behaviours in the lipid vesicles that can be experimentally evidenced with the techniques used in this work. This is very important because the use of these techniques allows knowing a priori if a peptide will have an antibacterial effect or not.

In general, the mechanisms of action proposed for antimicrobial peptides so far have been mainly focused on the primary, secondary and quaternary structures of peptides and the charged nature of the pathogen membrane. However, very little is known regarding the possibility of forming transitory lipid rafts in the external leaflet of the cell membrane, which, eventually, could perturb the mechanical properties of the membrane induced by the electrostatic interaction with the peptides adsorbed on the cell membrane [91,92]. On the basis of our previously reported simulations, we proposed a four step mechanism for small-sized peptides [39]. This mechanism includes the following steps:

i) Peptide accumulation and induction of phospholipid segregation.
ii) Peptide protruding into lipid/membrane domains with a low charged phospholipid content.
iii) Membrane collapse and pore formation.
iv) Peptides transposition and recovery of the bilayer structure.

These steps are shown in a schematic way in Fig. 6 SI. Antimicrobial peptides might possess a random-coil conformation in water solution, but when they approach the bilayer/solution interface they could change into a folded conformation as a consequence of the variation in the electrical permittivity in the vicinity of the bilayer interface. Several authors have suggested that this situation occurs [11,12]. An initial consequence of peptide folding is the change in its amphipathicity, favouring its electrostatic interaction with the external leaflet of the cell

membrane rich in charged phospholipids [14,60,65]. Results reported here, as well as in our previous work, support the idea that this is a key step in the mechanism of action of these antimicrobial peptides as is briefly discussed below:

1. Strong electrostatic interactions between cationic peptides and phospholipids with net negative charge located in the external leaflet of the cell membrane could trigger the lipid aggregations on the membrane.
2. Peptides adsorbed on the surface of the lipid bilayer do not protrude into lipid bilayers with a high proportion of charged phospholipids, as a consequence of the strong electrostatic interactions between peptides and charged phospholipids (as depicted in Fig. 6).
3. The stiffness of the lipid bilayer (associated with its bending modulus) is a property that depends on its lipid composition. In general, this stiffness increases with the lipid charge content. Thus, an increase in the ratio of charged lipids induces an increase of the bending modulus of the membrane, and hence also enhances the mechanical stability of the membrane. On the one hand, the formation of lipid aggregates (or lipid rafts) in the membrane, as a consequence of the strong electrostatic interactions between cationic peptides and anionic phospholipids, induces the emergence of inhomogeneities in the bending modulus of the membrane. This can trigger the disruption of the membrane due to the abrupt variation of its bending modulus along the frontier between phospholipid rafts with different composition.

Although all the steps are important, the results obtained in this study indicate that some processes are crucial for this mechanism of action. Peptide discrimination between pathogens and host cells is apparently due to electrostatic interactions between the cationic peptides and negative phospholipids forming the external leaflet of the pathogen membrane, and previous simulations showed that the lytic activity of these peptides must be preceded by a phospholipid segregation [39]. As a consequence of this phospholipid segregation (induced by the presence of charged peptides in the vicinity of the membrane), mechanical inhomogeneities appear in the membrane, promoting membrane rupture when a threshold concentration of peptides adsorbed on the membrane is achieved. This explains the high structural demand for these peptides to maintain a delicate balance between the affinity for the bilayer surface, a low peptide-peptide repulsion (in order to reach the threshold concentration) and an acceptable tendency to penetrate into the bilayer. Therefore, our results suggest that the lytic effect of small cationic peptides should be considered as a dynamic picture of structural transformations adopted by the lipid–peptide mixture depending on the relative ratio of the two species, rather than a static picture of pores induced in the membrane by the presence of peptides.

5. Conclusions

The results obtained in this study allow us to draw important conclusions on two different aspects: i) a better understanding of the mechanism of action of small-sized peptides as antibacterial agents, ii) the possible pharmacophoric requirement for these small-sized peptides

i Our results (theoretical and experimental) indicate that small sized peptides have a particular mechanism of action that is different to that of large peptides. These results support a previously proposed four step mechanism of action [39]. It is important to remark that in this process, the ability to reach a threshold concentration of peptides, and thus probably a non-monomeric state, is a key step for a successful outcome. Consequently, this mechanism explains the importance of maintaining a delicate balance between affinity for the bilayer surface, a low peptide-peptide repulsion (in order to reach the threshold concentration) and an acceptable tendency to penetrate the bilayer.

ii It has previously been proposed that a sequence with at least 3 R and 3 W is a minimum structural requirement for these short peptides to become a “pharmacophore” [24]. Our results are in line with this proposal and include an important addition. This study shows that for such 9 amino acid long peptides, a net charge of +4 is the optimal for producing antibacterial activity. The information reported in this study is very important for designing new antibacterial peptides with these structural characteristics.

Declaration of competing interest

The authors declare that they have no known competing financial interests or personal relationships that could have appeared to influence the work reported in this paper.

Acknowledgments

RDE and ADG acknowledge the continued support of UNSL-Argentina. BL, RDE, ADG and GEF ar researchers of CONICET.

Funding

This work was partially supported by ANPCyT -Argentina (PICT-2018- 03259), CICITCA-UNSJ, Argentina. This work has also been partially financed through projects 20933/PI/18 (financed by Fundación Seneca-Murcia-España) and CTQ2017-87708-R (financed by the Ministry of Economy, Industry, and Commerce of Spain). This work was also funded by grants provided by the Hungarian Momentum programme (LP2016-2), by the National Competitiveness and Excellence Program, Hungary (NVKP_16-1-2016-0007), and by the BIONANO_GINOP-2.3.2-15-2016-00017 project.

Appendix A. Supplementary data

Supplementary data to this article can be found online at https://doi.org/10.1016/j.bbamem.2021.183665.

References

[1] C. Lee, M. Ventola, The antibiotic resistance crisis part 1: causes and threats, Pharm. Ther. 40 (4) (2014) 277–283.
[2] H. Stower, Antibiotic tolerance leads to antibiotic resistance, Nat. Med. 26 (2) (2020) 163. Internet. Available from, https://doi.org/10.1038/s41591-020-0778-7.
[3] R.D. Enriz, F.D. Suvire, S.A. Andujar, M.A. Alvarez, M. Vettorazzi, J.G. Dolab, et al., The long and winding road to convert an antimicrobial compound into an antimicrobial drug: an overview from a medicinal chemistry point of view, Curr. Org. Chem. 21 (18) (2017) 1885–1895.
[4] G. Annunziato, G. Costantino, Antimicrobial peptides (AMPs): a patent review (2015-2020), Expert Opin. Ther. Pat. 0 (0) (2020), https://doi.org/10.1080/13543776.2020.1851679 [Internet]. Available from:.
[5] K. Hiramatsu, N. Aritaka, H. Hanaki, S. Kawasaki, Y. Hosoda, S. Hori, et al., Dissemination in Japanese hospitals of strains of Staphylococcus aureus heterogeneously resistant to vancomycin, Lancet 350 (9092) (1997) 1670–1673. Dec 6.
[6] M.L. Cohen, Epidemiology of drug resistance: implications for a post—antimicrobial era, Science (80-) 257 (5073) (1992 Aug 21) [Internet]. 1050 LP – 1055. Available from: http://science.sciencemag.org/content/257/5073/1050.abstract.
[7] A.H. Siddiqui JK, Methicillin Resistant *Staphylococcus aureus*, StatPearls Publishing, Treasure Island (FL), 2020.
[8] G. Taubes, The bacteria fight back, Science (80-) 321 (5887) (2008 Jul 18) 356–361 [Internet]. Available from: http://science.sciencemag.org/content/321/5887/356.abstract.
[9] M. Zasloff, Antimicrobial peptides in health and disease, N. Engl. J. Med. 10 (347) (2002) 1199–1200.
[10] M. Zasloff, Antimicrobial peptides of multicellular organisms, Nature 415 (6870) (2002) 389–395. Internet. Jan 24. Available from, http://www.ncbi.nlm.nih.gov/pubmed/11807545.
[11] F.H. Waghu, L. Gopi, R.S. Barai, P. Ramteke, B. Nizami, S. Idicula-Thomas, CAMP: collection of sequences and structures of antimicrobial peptides, Nucleic Acids Res. 42 (D1) (2014) D1154–D1158. Internet. Jan 1. Available from, https://doi.org/10.1093/nar/gkt1157.

[12] M. Magana, M. Pushpanathan, A.L. Santos, L. Leanse, M. Fernandez, A. Ioannidis, et al., The value of antimicrobial peptides in the age of resistance, Lancet Infect. Dis. 20 (9) (2020) e216–e230. Internet. Available from, https://doi.org/10.1016/S1473-3099(20)30327-3.
[13] K.A. Brogden, Antimicrobial peptides: pore formers or metabolic inhibitors in bacteria? Nat. Rev. Microbiol. 3 (3) (2005) 238–250.
[14] E.H. Mattar, H.A. Almehdar, H.A. Yacoub, V.N. Uversky, E.M. Redwan, Antimicrobial potentials and structural disorder of human and animal defensins, Cytokine Growth Factor Rev. 28 (2016) 95–111. Internet. Available from, http://www.sciencedirect.com/science/article/pii/S1359610115300071.
[15] F. Zsila, S. Bősze, K. Horváti, I.C. Szigyártó, T. Beke-Somfai, Drug and dye binding induced folding of the intrinsically disordered antimicrobial peptide CM15, RSC Adv. 7 (65) (2017) 41091–41097. Internet. Available from, https://doi.org/10.1039/C7RA05290A.
[16] S.E. Blondelle, K. Lohner, M.-I. Aguilar, Lipid-induced conformation and lipid-binding properties of cytolytic and antimicrobial peptides: determination and biological specificity, Biochim. Biophys. Acta Biomembr. 1462 (1–2) (1999) 89–108. Dec.
[17] S.E. Blondelle, B. Forood, R.A. Houghten, E. Pérez-Payá, Secondary structure induction in aqueous vs membrane-like environments, Biopolymers 42 (4) (1997) 489–498. Oct 5.
[18] D. Sengupta, H. Leontiadou, A.E. Mark, S.-J. Marrink, Toroidal pores formed by antimicrobial peptides show significant disorder, Biochim. Biophys. Acta Biomembr. 1778 (10) (2008) 2308–2317 [Internet]. Available from: http://www.sciencedirect.com/science/article/pii/S0005273608001764.
[19] T.-H. Lee, N. Hall K, M.-I. Aguilar, Antimicrobial peptide structure and mechanism of action: a focus on the role of membrane structure, Curr. Top. Med. Chem. 16 (1) (2015) 25–39.
[20] J.K. Boparai, P.K. Sharma, Mini review on antimicrobial peptides, sources, mechanism and recent applications, Protein Pept. Lett. 27 (1) (2019) 4–16.
[21] G. Wang, X. Li, Z. Wang, APD2: the updated antimicrobial peptide database and its application in peptide design, Nucleic Acids Res. 37 (Suppl. 1) (2009) 933–937.
[22] O. Parravicini, C. Somlai, S.A. Andujar, A.D. Garro, B. Lima, A. Tapia, et al., Small peptides derived from penetratin as antibacterial agents, Arch. Pharm. (Weinheim) 349 (4) (2016) 242–251.
[23] A.D. Garro, M.S. Olivella, J.A. Bombasaro, B. Lima, A. Tapia, G. Feresin, et al., Penetratin and derivatives acting as antibacterial agents, Chem. Biol. Drug Des. 82 (2) (2013) 167–177.
[24] A.D. Garro, F.M. Garibotto, A.M. Rodriguez, M. Raimondi, S.A. Zacchino, A. Perczel, et al., New small-size antifungal peptides: design, synthesis and antifungal activity, Lett. Drug Des. Discovery 8 (6) (2011) 562–567.
[25] M.S. Olivella, A.M. Rodriguez, S.A. Zacchino, C. Somlai, B. Penke, V. Farkas, et al., New antifungal peptides. Synthesis, bioassays and initial structure prediction by CD spectroscopy, Bioorg. Med. Chem. Lett. 20 (16) (2010) 4808–4811.
[26] F.M. Garibotto, A.D. Garro, M.F. Masman, A.M. Rodriguez, P.G.M.M. Luiten, M. Raimondi, et al., New small-size peptides possessing antifungal activity, Bioorg. Med. Chem. 18 (1) (2010) 158–167 [Internet]. Available from, https://doi.org/10.1016/j.bmc.2009.11.009.
[27] M.F. Masman, A.M. Rodriguez, M. Raimondi, S.A. Zacchino, P.G.M. Luiten, C. Somlai, et al., Penetratin and derivatives acting as antifungal agents, Eur. J. Med. Chem. 44 (1) (2009) 212–228.
[28] F.M. Garibotto, A.D. Garro, A.M. Rodriguez, M. Raimondi, S.A. Zacchino, A. Perczel, et al., Penetratin analogues acting as antifungal agents, Eur. J. Med. Chem. 46 (1) (2011) 370–377.
[29] Z. Khurshid, M.S. Zafar, M. Naseem, R.S. Khan, S. Najeeb, Human oral defensins antimicrobial peptides: a future promising antimicrobial drug, Curr. Pharm. Des. 24 (10) (2018) 1130–1137.
[30] C. Verma, S. Seebah, S.M. Low, L. Zhou, S.P. Liu, J. Li, et al., Defensins: antimicrobial peptides for therapeutic development, Biotechnol. J. 2 (11) (2007) 1353–1359.
[31] T. Ganz, Defensins: antimicrobial peptides of innate immunity, Nat. Rev. Immunol. 3 (9) (2003) 710–720.
[32] E. Jamasbi, A. Mularski, F. Separovic, Model membrane and cell studies of antimicrobial activity of melittin analogues, Curr. Top. Med. Chem. 16 (2016) 40–45.
[33] K.S. Usachev, S.V. Efimov, O.A. Kolosova, E.A. Klochkova, A.V. Aganov, V. V. Klochkov, Antimicrobial peptide protegrin-3 adopt an antiparallel dimer in the presence of DPC micelles: a high-resolution NMR study, J. Biomol. NMR 62 (1) (2015) 71–79 [Internet]. Available from, https://doi.org/10.1007/s10858-015-9920-0.
[34] P.M. Fischer, N.Z. Zhelev, S. Wang, J.E. Melville, R. Fahraeus, D.P. Lane, Structure-activity relationship of truncated and substituted analogues of the intracellular delivery vector Penetratin, J. Pept. Res. 55 (2) (2000) 163–172.
[35] A. Czajlik, E. Mesko, B. Penke, A. Perczel, Investigation of penetratin peptides. Part 1. The environment dependent conformational properties of penetratin and two of its derivatives, J. Pept. Sci. 8 (4) (2002) 151–171.
[36] W.L. Zhu, S.Y. Shin, Antimicrobial and cytolytic activities and plausible mode of bactericidal action of the cell penetrating peptide penetratin and its Lys-linked two-stranded peptide, Chem. Biol. Drug Des. 73 (2) (2009) 209–215.
[37] J.S. Bahnsen, H. Franzyk, A. Sandberg-Schaal, H.M. Nielsen, Antimicrobial and cell-penetrating properties of penetratin analogs: effect of sequence and secondary structure, Biochim. Biophys. Acta Biomembr. 1828 (2) (2013) 223–232.
[38] Z. Liu, A. Brady, A. Young, B. Rasimick, K. Chen, C. Zhou, et al., Length effects in antimicrobial peptides of the (RW)n series, Antimicrob. Agents Chemother. 51 (2) (2007 Feb) 597–603 [Internet]. 2006/12/04. Available from: https://pubmed.ncbi.nlm.nih.gov/17145799.
[39] J.J. Lopez Cascales, A. Garro, R.D. Porasso, R.D. Enriz, The dynamic action mechanism of small antimicrobial peptides, Phys. Chem. Chem. Phys. 16 (39) (2014) 21694–21705.
[40] P. Wayne, CLSI, Performance Standards for Antimicrobial Susceptibility Testing, Twenty-second Informational Supplement. CLSI document M100-S22, Clinical and Laboratory Standards Institute, 2012.
[41] M. Ardhammar, P. Lincoln, B. Nordén, Invisible liposomes: refractive index matching with sucrose enables flow dichroism assessment of peptide orientation in lipid vesicle membrane, Proc. Natl. Acad. Sci. 99 (24) (2002 Nov 26) 15313–15317 [Internet]. Available from: http://www.pnas.org/content/99/24/15313.abstract.
[42] J.J. Lopez Cascales, S. Zenak, J. Garcia De La Torre, O.G. Lezama, A. Garro, R. D. Enriz, Small cationic peptides: influence of charge on their antimicrobial activity, ACS Omega 3 (5) (2018) 5390–5398.
[43] H.J.C. Berendsen, J.P.M. Postma, W.F. van Gunsteren, HJ. Interaction models for water in relation to protein hydration, in: B. Pullman (Ed.), Intermolecular Forces. The Jerusa, Intermolecular Forces, 1981, pp. 331–342.
[44] H.J.C. Berendsen, D. van der Spoel, R. van Drunen, GROMACS: a message-passing parallel molecular dynamics implementation, Comput. Phys. Commun. 91 (1–3) (1995) 43–56 [Internet]. Available from: www.scopus.com.
[45] E. Lindahl, B. Hess, D. van der Spoel, GROMACS 3.0: a package for molecular simulation and trajectory analysis, J. Mol. Model. 7 (8) (2001) 306–317.
[46] H.J.C. Berendsen, J.P.M. Postma, W.F. van Gunsteren, A. DiNola, J.R. Haak, Molecular dynamics with coupling to an external bath, J. Chem. Phys. 81 (8) (1984) 3684–3690 [Internet]. Available from: www.scopus.com.
[47] A. Seeling, J. Seeling, The dynamic structure of fatty acyl chains in a phospholipid bilayer measured by deuterium magnetic resonance, Biochemistry 23 (23) (1974) 4839–4845.
[48] T. Darden, D. York, L. Pedersen, Particle mesh Ewald: an N log(N) method for Ewald sums in large systems, J. Chem. Phys. 98 (12) (1993) 10089–10092 [Internet]. Available from: www.scopus.com.
[49] U. Essmann, L. Perera, M.L. Berkowitz, T. Darden, H. Lee, L.G. Pedersen, A smooth particle mesh Ewald method, J. Chem. Phys. 103 (19) (1995) 8577–8593.
[50] B. Hess, H. Bekker, H.J.C. Berendsen, J.G.E.M. Fraaije, H.J.C. Fraaije, LINCS: a linear constraint solver for molecular simulations, J. Comput. Chem. 18 (12) (1997) 1463–1472 [Internet]. Available from: www.scopus.com.
[51] N. Schmid, A.P. Eichenberger, A. Choutko, S. Riniker, M. Winger, A.E. Mark, et al., Definition and testing of the GROMOS force-field versions 54A7 and 54B7, Eur. Biophys. J. 40 (7) (2011) 843–856.
[52] K.H. Park, Y.H. Nan, Y. Park, J.I. Kim, I.-. Park, K.-. Hahm, et al., Cell specificity, anti-inflammatory activity, and plausible bactericidal mechanism of designed Trp-rich model antimicrobial peptides, Biochim. Biophys. Acta Biomembr. 1788 (5) (2009) 1193–1203.
[53] A. Hawrani, R.A. Howe, T.R. Walsh, C.E. Dempsey, Origin of low mammalian cell toxicity in a class of highly active antimicrobial amphipathic helical peptides, J. Biol. Chem. 283 (27) (2008) 18636–18645. Internet. Jul 4 [cited 2020 Dec 26. Available from, http://www.jbc.org/cgi/content/short/283/27/18636.
[54] B. Findlay, G.G. Zhanel, F. Schweizer, Cationic amphiphiles, a new generation of antimicrobials inspired by the natural antimicrobial peptide scaffold, Antimicrob. Agents Chemother. 54 (10) (2010) 4049–4058.
[55] A. Walrant, I. Correia, C.-Y. Jiao, O. Lequin, E.H. Bent, N. Goasdoué, et al., Different membrane behaviour and cellular uptake of three basic arginine-rich peptides, Biochim. Biophys. Acta Biomembr. 1808 (1) (2011) 382–393 [Internet]. Available from: http://www.sciencedirect.com/science/article/pii/S000527361000324X.
[56] R.W. Woody, Contributions of tryptophan side chains to the far-ultraviolet circular dichroism of proteins, Eur. Biophys. J. 23 (4) (1994) 253–262. Internet. Available from, https://doi.org/10.1007/BF00213575.
[57] V.V. Andrushchenko, H.J. Vogel, E.J. Prenner, Solvent-dependent structure of two tryptophan-rich antimicrobial peptides and their analogs studied by FTIR and CD spectroscopy, Biochim. Biophys. Acta Biomembr. 1758 (10) (2006) 1596–1608 [Internet]. Available from, http://www.sciencedirect.com/science/article/pii/S0005273606002902.
[58] A.S. Ladokhin, M.E. Selsted, S.H. White, CD spectra of indolicidin antimicrobial peptides suggest turns, not polyproline helix, Biochemistry 38 (38) (1999) 12313–12319.
[59] S. Nagpal, V. Gupta, K.J. Kaur, D.M. Salunke, Structure-function analysis of tritrypticin, an antibacterial peptide of innate immune origin, J. Biol. Chem. 274 (33) (1999) 23296–23304.
[60] Locock KES, Bioinspired polymers: antimicrobial polymethacrylates, Aust. J. Chem. 69 (7) (2016) 717–724 [Internet]. Available from, https://doi.org/10.1071/CH16047.
[61] R.W. Woody, Circular dichroism of intrinsically disordered proteins, in: V. U. Longhi, S (Eds.), Instrumental Analysis of Intrinsically Disordered Proteins: Assesing Structure and Conformation [Internet], John Wiley & Sons, Inc., 2010, pp. 303–321. Available from, https://www.disprot.org/.
[62] N. Amdursky, M.M. Stevens, Circular dichroism of amino acids: following the structural formation of phenylalanine, ChemPhysChem 16 (13) (2015) 2768–2774. Internet. Sep 14. Available from, https://doi.org/10.1002/cphc.201500260.
[63] N. Vladimir, S.L. Uversky, in: V.N.U.S. Longhi (Ed.), Instrumental Analysis of Intrinsically Disordered Proteins: Assessing Structure and Conformation, John Wiley & Sons, Inc., 2010.
[64] A. Barth, Infrared spectroscopy of proteins, Biochim. Biophys. Acta Bioenerg. 1767 (9) (2007) 1073–1101.
[65] A. Dong, J. Matsuura, M.C. Manning, J.F. Carpenter, Intermolecular beta-sheet results from trifluoroethanol-induced nonnative alpha-helical structure in beta-sheet predominant proteins: infrared and circular dichroism spectroscopic study,

Arch. Biochem. Biophys. 355 (2) (1998) 275–281. Internet. Available from, http://europepmc.org/abstract/MED/9675038.
[66] M.R. Yeaman, N.Y. Yount, Mechanisms of antimicrobial peptide action and resistence, Pharmacol. Rev. 55 (1) (2003 Mar) 27–55 [Internet]. Available from: http://www.ncbi.nlm.nih.gov/pubmed/12615953.
[67] A.S. Ladokhin, Evaluation of lipid exposure of tryptophan residues in membrane peptides and proteins, Anal. Biochem. 276 (1) (1999) 65–71.
[68] M. Ardhammar, N. Mikati, B. Nordén, Chromophore orientation in liposome membranes probed with flow dichroism, J. Am. Chem. Soc. 120 (38) (1998) 9957–9958. Internet. Sep 1. Available from, https://doi.org/10.1021/ja981102g.
[69] A. Rodger, J. Rajendra, R. Marrington, M. Ardhammar, B. Nordén, J.D. Hirst, et al., Flow oriented linear dichroism to probe protein orientation in membrane environments, Phys. Chem. Chem. Phys. 4 (16) (2002) 4051–4057. Internet. Available from, https://doi.org/10.1039/B205080N.
[70] B.N. Alison Rodger, TD, Linear Dichroism and Circular Dichroism. A Textbook on Polarized-Light Spectroscopy, RSC Publishing, Cambridge, 2010.
[71] F.R. Svensson, P. Lincoln, B. Nordén, E.K. Esbjörner, Tryptophan orientations in membrane-bound gramicidin and melittin—a comparative linear dichroism study on transmembrane and surface-bound peptides, Biochim. Biophys. Acta Biomembr. 1808 (1) (2011) 219–228 [Internet]. Available from: http://www.sciencedirect.com/science/article/pii/S0005273610003585.
[72] M. Kogan, B. Feng, B. Nordén, S. Rocha, T. Beke-Somfai, Shear-induced membrane fusion in viscous solutions, Langmuir 30 (17) (2014) 4875–4878. Internet. May 6. Available from, https://doi.org/10.1021/la404857r.
[73] S. Rocha, M. Kogan, T. Beke-Somfai, B. Nordén, Probing microscopic orientation in membranes by linear Dichroism, Langmuir 32 (12) (2016) 2841–2846. Internet. Mar 29. Available from, https://doi.org/10.1021/acs.langmuir.5b04229.
[74] M.R. Hicks, A. Damianoglou, A. Rodger, T.R. Dafforn, Folding and membrane insertion of the pore-forming peptide gramicidin occur as a concerted process, J. Mol. Biol. 383 (2) (2008) 358–366. Internet. Available from, http://www.sciencedirect.com/science/article/pii/S0022283608009716.
[75] Caesar CEB, E.K. Esbjörner, P. Lincoln, B. Nordén, Membrane interactions of cell-penetrating peptides probed by tryptophan fluorescence and dichroism techniques: correlations of structure to cellular uptake, Biochemistry 45 (24) (2006) 7682–7692. Internet. Jun 1. Available from, https://doi.org/10.1021/bi052095t.
[76] C.E.B. Brattwall, P. Lincoln, B. Nordén, Orientation and conformation of cell-penetrating peptide Penetratin in phospholipid vesicle membranes determined by polarized-light spectroscopy, J. Am. Chem. Soc. 125 (47) (2003) 14214–14215.
[77] W. Hu, K.C. Lee, T.A. Cross, Tryptophans in membrane proteins: Indole ring orientations and functional implications in the gramicidin channel, Biochemistry 32 (27) (1993) 7035–7047. Internet. Jul 1. Available from, https://doi.org/10.1021/bi00078a032.
[78] M. Schiffer, C.H. Chang, F.J. Stevens, The functions of tryptophan residues in membrane proteins, Protein Eng. Des. Sel. 5 (3) (1992) 213–214.
[79] W.M. Shafer, F. Hubalek, M. Huang, J. Pohl, Bactericidal activity of a synthetic peptide (CG 117-136) of human lysosomal cathepsin G is dependent on arginine content, Infect. Immun. 64 (11) (1996) 4842–4845 [Internet]. Nov. Available from, https://pubmed.ncbi.nlm.nih.gov/8890249.
[80] E. Egberts, S.J. Marrink, H.J.C. Berendsen, Molecular-dynamics simulation of a phospholipid membrane, Eur. Biophys. J. 22 (6) (1994) 423–436.
[81] G.M. Torrie, J.P. Valleau, Nonphysical sampling distributions in Monte Carlo free-energy estimation: umbrella sampling, J. Comput. Phys. 23 (2) (1977) 187–199. Internet. Available from, http://www.sciencedirect.com/science/article/pii/0021999177901218.
[82] S. Kumar, D. Bouzida, R.H. Swendsen, P.A. Kollman, J.M. Rosenberg, The weighted histogram analysis method for free-energy calculations on biomolecules. I. the method, J. Comput. Chem. 13 (8) (1992) 1011–1021 [Internet]. Oct 1. Available from, https://doi.org/10.1002/jcc.540130812.
[83] M.B. Strøm, B.E. Haug, Ø. Rekdal, M.L. Skar, W. Stensen, J.S. Svendsen, Important structural features of 15-residue lactoferricin derivatives and methods for improvement of antimicrobial activity, Biochem. Cell Biol. 80 (1) (2002 Feb 1) 65–74 [Internet]. Available from: https://doi.org/10.1139/o01-236.
[84] M.B. Strøm, B.E. Haug, M.L. Skar, W. Stensen, T. Stiberg, J.S. Svendsen, The pharmacophore of short cationic antibacterial peptides, J. Med. Chem. 46 (9) (2003) 1567–1570 [Internet]. Apr 1. Available from, https://doi.org/10.1021/jm0340039.
[85] Y. Shai, Mode of action of membrane active antimicrobial peptides, Biopolym. Pept. Sci. Sect. 66 (4) (2002 Jan 1) 236–248 [Internet]. Available from: https://doi.org/10.1002/bip.10260.
[86] M.P. Aliste, D.P. Tieleman, Computer simulation of partitioning of ten pentapeptides ace-WLXLL at the cyclohexane/water and phospholipid/water interfaces, BMC Biochem. 6 (1) (2005) 30 [Internet]. Available from: https://doi.org/10.1186/1471-2091-6-30.
[87] J.E. Johnson, N.M. Rao, S.-W. Hui, R.B. Cornell, Conformation and lipid binding properties of four peptides derived from the membrane-binding domain of CTP: phosphocholine cytidylyltransferase, Biochemistry 37 (26) (1998) 9509–9519. Internet. Jun 1. Available from, https://doi.org/10.1021/bi980340l.
[88] F.Y. Chen, M.T. Lee, H.W. Huang, Sigmoidal concentration dependence of antimicrobial peptide activities: a case study on alamethicin, Biophys. J. 82 (2) (2002) 908–914. Internet. Available from, https://doi.org/10.1016/S0006-3495(02)75452-0.
[89] V. Teixeira, M.J. Feio, M. Bastos, V. Texeira, M.J. Feio, M. Bastos, Role of lipids in the interaction of antimicrobial peptides with membranes, Prog. Lipid Res. 51 (2) (2012) 149–177. Internet. Apr. Available from, https://linkinghub.elsevier.com/retrieve/pii/S0163782711000518.
[90] Y. Shai, Mechanism of the binding, insertion and destabilization of phospholipid bilayer membranes by α-helical antimicrobial and cell non-selective membrane-lytic peptides, Biochim. Biophys. Acta Biomembr. 1462 (1–2) (1999) 55–70.
[91] A.A. Polyansky, P.E. Volynsky, A.S. Arseniev, R.G. Efremov, Adaptation of a membrane-active peptide to heterogeneous environment. II. The role of mosaic nature of the membrane surface, J. Phys. Chem. B 113 (4) (2009) 1120–1126.
[92] K.L.H. Lam, H. Wang, T.A. Siaw, M.R. Chapman, A.J. Waring, J.T. Kindt, et al., Mechanism of structural transformations induced by antimicrobial peptides in lipid membranes, Biochim. Biophys. Acta Biomembr. 1818 (2) (2012) 194–204 [Internet]. Available from: http://www.sciencedirect.com/science/article/pii/S0005273611003890.